AD-A169 237 MICROMETEOROLOGICAL TRANSITIONS IN THE MORNING BOUNDARY LAYER OVER ROLLING TERRAIN(U) NORTH CAROLINA STATE UNIV AT RALEIGH A J RIORDAN ET AL. 20 MAR 86 ARO-19649.3-05 1/1

UNCLASSIFIED DAAG29-82-K-0183 F/G 4/2 NL

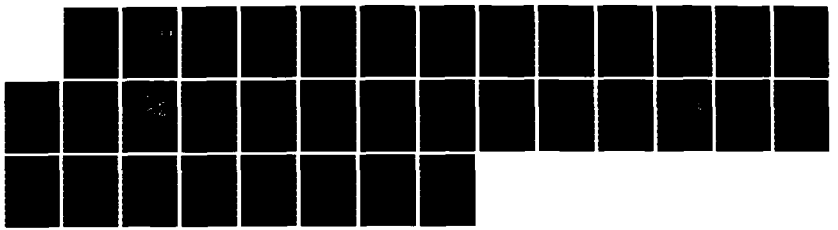

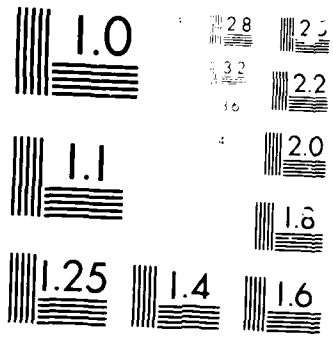
1.0
2.8
2.2
2.0
1.8
1.1
1.25
1.4
1.6

MICROMETEOROLOGICAL TRANSITIONS IN THE MORNING BOUNDARY LAYER OVER ROLLING TERRAIN

FINAL REPORT

ALLEN J. RIORDAN
JERRY M. DAVIS

MARCH 1986

U. S. ARMY RESEARCH OFFICE

GRANT NUMBER DAAG29-82-K-0183

NORTH CAROLINA STATE UNIVERSITY
RALEIGH, NORTH CAROLINA

APPROVED FOR PUBLIC RELEASE:
DISTRIBUTION UNLIMITED

MASTER COPY - FOR REPRODUCTION PURPOSES

UNCLASSIFIED
SECURITY CLASSIFICATION OF THIS PAGE (When Data Entered)

REPORT DOCUMENTATION PAGE		READ INSTRUCTIONS BEFORE COMPLETING FORM
1. REPORT NUMBER ARO 19649.3-GS	2. GOVT ACCESSION NO. N/A	3. RECIPIENT'S CATALOG NUMBER N/A
4. TITLE (and Subtitle) Micrometeorological Transitions in the Morning Boundary Layer Over Rolling Terrain		5. TYPE OF REPORT & PERIOD COVERED Final Report 1982-1985 6. PERFORMING ORG. REPORT NUMBER
7. AUTHOR(s) Allen J. Riordan Jerry M. Davis		8. CONTRACT OR GRANT NUMBER(s) DAAG29-82-K-0183
9. PERFORMING ORGANIZATION NAME AND ADDRESS North Carolina State University Raleigh, NC		10. PROGRAM ELEMENT, PROJECT, TASK AREA & WORK UNIT NUMBERS
11. CONTROLLING OFFICE NAME AND ADDRESS U. S. Army Research Office Post Office Box 12211 Research Triangle Park, NC 27709		12. REPORT DATE 20 March 1986 13. NUMBER OF PAGES 5
14. MONITORING AGENCY NAME & ADDRESS(if different from Controlling Office)		15. SECURITY CLASS. (of this report) Unclassified 15a. DECLASSIFICATION/DOWNGRADING SCHEDULE

16. DISTRIBUTION STATEMENT (of this Report)

Approved for public release; distribution unlimited.

17. DISTRIBUTION STATEMENT (of the abstract entered in Block 20, if different from Report)

NA

18. SUPPLEMENTARY NOTES

The view, opinions, and/or findings contained in this report are those of the author(s) and should not be construed as an official Department of the Army position, policy, or decision, unless so designated by other documentation.

19. KEY WORDS (Continue on reverse side if necessary and identify by block number)

inversion
inversion breakdown
inversion, synoptic control
modeling inversion breakdown
morning transition of inversion

20. ABSTRACT (Continue on reverse side if necessary and identify by block number)

Six years of temperature and wind data from two 60m micrometeorological towers in the piedmont of the Carolinas were analyzed. One tower was near a large lake, the other in mostly-forested terrain. Statistics of the basic tower measurements were generated and their time evolution was

DD FORM 1 JAN 73 1473 EDITION OF 1 NOV 65 IS OBSOLETE

UNCLASSIFIED
SECURITY CLASSIFICATION OF THIS PAGE (When Data Entered)

described for the morning transition period near sunrise. A stepwise regression model was developed and tested to predict the daily transition time at each site based on tower variables.

To determine large-scale influences on the local inversion and its morning transition, the local tower data from each site were then related to the synoptic-scale pressure field over the eastern one-third of the United States. To accomplish the comparison, an objective typing scheme was developed in which the gridded daily sea-level pressure field was expressed in terms of eigenvector types.

Results document the average morning transition sequence in terms of systematic changes in radiation, wind and temperatures. The regression models are quite similar at both sites and predict transition time with a least-squared regression of 0.76 for clear mornings at the forested site.

The eigenvector analysis successfully categorized each day's pressure field into ten types. These showed very close association with the local inversion intensity at sunrise, but had very little relation to morning transition time at each site.

List of Appendices

I. The Morning Inversion Near the Ground and Its Daytime Transition at Two rural Sites in the Carolinas

II. Exploration of Synoptic Influences on Inversion Strength and Transitions into the Daytime Boundary Layer (Abstract only)

The Problem

The nocturnal inversion is routinely observed over nearly all continental locations, and its development and growth has been widely observed, described and modeled. The breakdown of the inversion after sunrise, a routine event marking a transition of the planetary boundary layer from the stable nocturnal conditions to a well-mixed daytime state has been less studied.

Some studies have documented the morning transition for homogeneous terrain (Singer and Raynor, 1957; De Marrais, 1959; Clarke et al, 1971; Takle et al, 1976), but only a few have explored the transition for terrain that is more complex (Lenschow et al, 1979; Whiteman, 1982). Rarely has the transition for any terrain been documented for a data set large enough to approach a climatological basis.

The main objectives of the study were to:

1. Characterize the structure of the pre-dawn morning inversion and document its dissipation after sunrise. Variables to be studied included temperature gradient, stability, wind shear, standard deviation of the wind direction (σ_θ) and solar radiation.

2. Relate the daily breakdown of the morning inversion on the basis of time elapsed from local sunrise.

3. Identify locally-measured variables which could be used as predictors of the time required for inversion breakdown.

4. Evaluate the spatial representativeness of each site.

5. Determine the control of the pre-dawn inversion strength and morning transition time by the large-scale synoptic weather pattern.

Based on suggestions by proposal reviewers, detailed evaluations of nearby routine National Weather Service (NWS) soundings were included, statistics of σ_θ and Pasquill-Gifford-Turner stability were computed, and an objective analysis scheme was developed and used to define and classify the synoptic-scale weather pattern.

Six years of quality-controlled tower data from two dissimilar sites, one in rolling forrested terrain and the other by a large lake, were used in this study. One tower was located near the Shearon-Harris Nuclear Plant site 35 km southwest of Raleigh, North Carolina. The other site, by Lake Robinson, was located near the Robinson Nuclear Plant near Hartsville, South Carolina. Both sites had identical towers and instrumentation and both were maintained by meteorologists from the Carolina Power and Light Company.

Detailed discussions of methodology and results of this study can be found in:

Riordan, A.J., J. M. Davis, and R.B. Kiess, 1986: The morning inversion near the ground and its daytime transition at two rural sites in the Carolinas J. Clim. and Appl. Meteor. 25, 239-256.

Kiess, R.B., 1985: Exploration of synoptic influences on inversion strength and transitions into the daytime boundary layer. M.S. Thesis, North Carolina State University, Raleigh, N.C.

See the appendices to this report. These studies represent all reports published to date under this funding.

Important Results

Pre-dawn inversions in the 11 to 60m layer were found to exist on over 70% of the 1317 days with complete data at the land site, but were somewhat less frequent at the lake site. Once normalized to the time of local sunrise and sorted by the temperature difference, ΔT, between the 11 and 60m levels, the evolution of daytime conditions was quantitatively described. The inversion breakdown was found to be a well-ordered process. Mean temperature differences (ΔT), σ_θ at both tower levels, and wind shear evolve systematically.

New and interesting findings include the discovery that of all tower variables, ΔT is the best predictor of inversion breakdown. Once the data is sorted by cloudiness (as monitored indirectly by solar radiation thresholds), stepwise regression shows that the transition time at both sites is predicted best by ΔT in the hour before sunrise.

In this endeavor, clear and nonclear day models were developed to predict the time, t, from local sunrise until the temperature at both 11 and 60 m was the same. The models were developed using the standard stepwise regression procedure supplemented with the maximum R^2 (coefficient of multiple determination) improvement technique developed at the SAS Institute. This procedure does not attempt to find the single best model; rather, it seeks the best one-variable, two-variable, etc., model. The final models selected in the present case were those that had the least number of independent variables while maintaining a high R^2 value. The models developed are as follows:

(a) Shearon-Harris Nuclear Plant

Clear day

$$t = 0.9253 + 0.1731\ \overline{\Delta T} + 0.0220\ \overline{T}_i$$

$$R^2 = 0.76 \qquad N = 100$$

Nonclear day

$$t = 1.238 + 0.1843 \ \overline{\Delta T} + 0.0160 \ \overline{T}_d$$

$$R^2 = 0.31 \qquad N = 675$$

(b) Robinson Nuclear Plant

Clear day

$$t = 1.220 + 0.2350 \ \overline{\Delta T} - 0.0751 \ \overline{V}_u$$

$$R^2 = 0.55 \qquad N = 274$$

Nonclear day

$$t = 1.587 + 0.309 \ \overline{\Delta T} - 0.1414 \ \overline{V}_u$$

$$R^2 = 0.42 \qquad N = 681$$

where ΔT is the temperature difference, $\overline{T}_d$ is the dew point temperature, $\overline{V}_u$ is the wind speed at the 60 m level, and overbars denote the average for the hour immediately preceeding sunrise.

An examination of the residuals for each model gave no indication of model inappropriateness. Since the models were designed to be forecast models, this attribute required testing. The cross-validation procedure developed by Efron and Gong (1983) was used to carry out the test. The derived models can be used in conjunction with the data set employed in their development to give forecasts of the dependent variables. However this is hardly a true test of the forecasting potential of the model. To provide a better test, 10% of the data points were randomly extracted from each model, the model was reestimated using the stepwise procedure. The reestimated model was then used to forecast the dependent variable for the extracted data. This procedure was repeated ten times for each model. The average error for the models as a whole was 0.43 hours. Actually this error value differed little from that obtained when the original models were used in a forecast mode with the data used to derive them. The average error in that case was 0.42 hours. As a further check, the Shearon-Harris model was used in conjunction with the Robinson data and vice vrsa. It was found that for a given site the model developed for that site gave the best results.

It is interesting that in several ways the inversion and its morning transition are not strongly site-specific. For example: (1) the regression models independently developed and tested to predict the inversion breakdown at the two quite different sites are surprisingly similar. (2) the daily ΔT value at sunrise correlates quite strongly (0.71) between the two tower sites. This is surprising when one considers that at the lake site the pre-dawn inversion is strongly influenced by winds from the direction of the lake. It is even more surprising that when the inversion intensity at either tower is compared with the NWS sounding taken at Greensboro, North Carolina, a site of comparable distance from either tower, the daily correlation is poor. Careful analysis of the NWS data, however, strongly suggests that the poor correlation arises from the coarse resolution of the sounding data, rather than from any real inversion differences.

Synoptic typing of the gridded daily sea-level pressure field for the eastern third of the United States was successfully accomplished through eigenvector analysis. Ten patterns or types were developed representing the pressure field. The actual observed pressure field for each morning was then objectively correlated with the types. Results show a very strong relation between the synoptic type and pre-dawn ΔT at each site. The influence of the lake was immediately obvious with some synoptic types, and this influence stood out as the strongest and perhaps only major difference in synoptic influence from one site to the other.

A final surprising result emerging from the synoptic study is that the synoptic type has very little effect on the time required for the morning breakdown of the inversion. There are a few exceptions to this finding. The most notable exception occurs when a synoptic-scale low lies over West Virginia. For this type, the average time from sunrise until lapse conditions are established at the lake site is lengthened from 2.5 h (the average for all other types) to nearly 3.5 h. Why a similar delay is not also seen at the other site is not clear.

Future plans for the follow-up of this project are to complete a revision of Kiess' M.S. thesis for publication, and to publish a short contribution on σ_θ statistics at each site during nighttime, morning transition and daytime, with additional data classifications based on wind direction (lake vs. land winds) and bulk stability.

Participating Scientific Personnel

1. Allen J. Riordan — Associate Professor of Meteorology
2. Jerry M. DAvis — Professor of Meteorology
3. Raymond B. Kiess — Graduate Research Assistant
   Master of Science Degree earned while employed on this project.

Bibliography

Clarke,R.H., A.J.Dyer, R.R.Brook, D.G.Reid and A.J.Troup, 1971: The Wangara experiment: Boundary layer data, CSIRO Div.Meteor. Phys., Tech. Paper No. 19, 336pp. [NTIS No. N71-37838.]

DeMarrais,G.A., 1959: Wind-speed profiles at Brookhaven National Laboratory, J.Meteor. , 16, 181-190.

Efron,B., and G.Gong, 1983: A leisurely look at the bootstrap, the jackknife, and cross-validation. Amer. Statist. , 37, 36-48.

Lenschow,D.W., B.B.Stankov and L.Mahrt, 1979: The rapid morning boundary-layer transition. J.Atmos.Sci. ,36, 2108-2124.

Singer,I.A., and G.S.Raynor, 1957: Analysis of meteorological tower data, April 1950-March 1952, Brookhaven National Laboratory. BNL 461 (T-102). 74 pp. [ASTIA Document No. AD 133806.]

Takle,E.S., R.H. Shaw and H.C.Vaughan, 1976: Low level stability and pollutant-trapping potential for a rural area. J. Appl. Meteor., 15, 36-42.

Whiteman,C.D., 1982: Breakup of temperature inversions in deep mountain valley: PartI.Observations. J.Appl.Meteor. ,21, 270-289

Appendix I

The Morning Inversion Near the Ground and Its Daytime Transition at Two Rural Sites in the Carolinas

ALLEN J. RIORDAN, JERRY M. DAVIS AND RAYMOND B. KIESS

Department of Marine, Earth and Atmospheric Sciences, North Carolina State University, Raleigh, NC 27650

(Manuscript received 23 March 1985, in final form 3 September 1985)

ABSTRACT

Six years of tower data from two dissimilar sites in the eastern piedmont of the Carolinas are analyzed to yield a selective climatology of the lower portion of the morning inversion. Its transition to daytime conditions is then described and statistically modeled.

Both sites are in clearings surrounded by forest, but one site is in a valley by a lake, while the other, 175 km to the north, is on a low hilltop. Measurements of wind speed and direction, the standard deviation of wind direction, dew point, and temperature at 11 m, temperature difference (ΔT) between 11 and 60 m, plus solar radiation, were analyzed for an 8-h period starting from three hours before local sunrise each day for both locations.

Results show that predawn inversions characterize over 70% of the data and strong inversions of over 5°C per 100 m in the tower layer characterize 30% of the mornings at the hilltop site. At the valley site, strong inversions are less common, probably because of the proximity of the lake. There is a correlation of 0.71 in daily site-to-site ΔT at dawn. This suggests strong overall synoptic control of the local inversion frequency.

The transition to well-mixed conditions after sunrise depends chiefly on ΔT prior to sunrise. Analysis of mean trends in variables during the transition shows it is a remarkably well-ordered process. The time from sunrise to a mean isothermal state (between 11 and 60 m only) takes about 1 to 2 h.

Daily transition is predicted by a linear regression scheme based on predawn conditions and developed and tested separately at each site. Chief predictors are inversion intensity, dew point and 60 m wind speed. For cloudy mornings the rms error for the prediction time from sunrise to mean isothermal conditions is 0.3 h. For days with variable cloudiness, a rather unspectacular R^2 value of 0.3 to 0.4 is, nevertheless, statistically significant. A similarity in models at both sites is noted. In cloudless conditions the models are, in fact, nearly interchangeable.

1. Introduction

The breakdown of the surface-based nocturnal inversion and the subsequent establishment of the daytime mixed layer after sunrise is one of the most dramatic changes that routinely affects the planetary boundary layer. The changes in stability and the wind field accompanying this morning transition are of profound importance in governing a myriad of processes such as, for example, the dispersion of pollutants in the surface layer or the flux of latent and sensible heat into the lower atmosphere.

Over flat, homogeneous terrain, analysis of temperature and wind profiles near the surface has been used to document the morning transition (Singer and Raynor, 1957; DeMarrais, 1959; Clarke et al., 1971). A recent study by Takle (1983) and Takle et al. (1976) has provided a 6-year documentation of inversions and superadiabatic conditions near Ames, Iowa at a rural site of low vertical relief. While invaluable for describing the transition on what approaches a climatological basis, there is some question about how well results of these studies apply to terrain that is more complex.

Some of these more complex environments have been explored to a limited degree as, for example, in studies of the urban boundary layer and its contrast to surrounding rural conditions (DeMarrais, 1961; Bakeı et al., 1969; Godowitch et al., 1979), and in studies of rural boundary-layer transition in complex terrain (Lenschow et al., 1979; Whiteman, 1982). However, while most of these studies are based on detailed measurements and, therefore, provide a great deal of insight into physical processes on a case study basis, their temporal limitations make it difficult to generalize their findings.

One question always pertinent to micrometeorological studies over nonuniform terrain is how the local terrain influences the climatology of the site. For example, just as one could explore the influence of topography on nocturnal inversion structure or frequency, one could assess similar local site influences on the process of inversion breakdown. The purpose of this study is to use a relatively lengthy set of measurements to compare and contrast climatologically the morning inversion and its transition from nocturnal to superadiabatic conditions for two rather dissimilar rural sites. A second related objective is to develop and test a model to predict the onset of the establishment of the mixed layer given the meteorological variables measurable near the time of sunrise. Similarities

between the two sites and site-specific differences will be discussed.

2. Sites and instrumentation

Carolina Power and Light Company (CP&L) has maintained continuous meteorological measurements under supervision of staff meteorologists at several nuclear power plant sites in North and South Carolina.

Analysis of data from two such sites from 1976 through 1982 will be described in this study. One site near the construction area for the Shearon-Harris Nuclear Plant (SHNP) is located in mostly forested rolling terrain 35 km southwest of Raleigh, North Carolina. The other is located near the shore of Lake Robinson at the Robinson Nuclear Plant (RNP) near Hartsville, South Carolina. These sites were chosen because quality-controlled data were available over extended time periods providing nearly continuous measurements. Both sites are close enough to each other to be largely influenced by the same synoptic regime. However, the sites differ since one is in a valley by a large lake and the other is on a low hilltop.

Nearly identical facilities were installed at both sites. This included a guyed, triangular, open-lattice tower supporting two levels of instrumentation. Wind speed, wind direction and its standard deviation (σ_θ) were measured at 12.5 and 61.4 m above the ground by mechanical cup–vane systems manufactured by Meteorological Research Inc. (MRI model 1074-22). Directional standard deviation was processed by an MRI Sigma Meter (No. 13074). A high-pass filter allowed signals to be passed above 0.0025 Hz over an 180 sec sampling interval. Aspirated single-element temperature sensors (Rosemount model 104ABG-1) were positioned at 11.0 m to measure the ambient temperature. Twin, redundant temperature-difference sensors (Rosemount model 104ABG-2) were mounted at 11.0 and 59.9 m and were operated simultaneously. At SHNP the dew point was measured at 12.5 and 61.4 m by Cambridge dew point sensors (EG&G International, Inc. model 110) and at both SHNP and RNP Honeywell lithium chloride type sensors (model SSP029D021) were mounted at 11.0 m. Solar pyranometers (Epply Laboratory model 8-48) were mounted near the towers at 1.5 m above the ground.

The wind sensors were mounted on horizontal booms projecting 2.1 m southeastward from the towers. The temperature probes and the lithium chloride sensor were housed in Climet (model 016) aspirated shields mounted on booms projecting westward from the towers.

Westinghouse Environmental Monitoring Systems were used for data logging at each site. They continuously converted sensor outputs to a proportional number of discrete pulses that were electrically integrated and recorded on magnetic tape in 15-min averaging periods.

A routine onsite maintenance and calibration program as required by Nuclear Regulatory Guide 1.23 was strictly maintained throughout the 1976–82 study period. On a semiannual basis:

(i) both wind systems were changed and replaced with NBS-traceable calibrated sensors;

(ii) ambient and differential temperature systems were changed and replaced with NBS-traceable calibrated systems;

(iii) the Cambridge dew point system and the bobbin element in the lithium chloride sensor were changed; and

(iv) the calibration of the pyranometer was checked. The sensor was changed annually.

Instruments were moved from site to site following calibration. Interim calibrations of all systems were performed at intervals of six weeks or less and comparison of the output of the twin, redundant delta-temperature systems, received in real time at a meteorological center maintained by CP&L, at Raleigh helped ensure that discrepancies in temperature differences were detected and corrected rapidly.

Table 1 lists the sensor errors for each component discussed in this study. It is difficult to quantify the total errors of the measurement system because of the conversion of sensor output to discrete pulses. For instance, the system accuracy, including effects of processor and data logger errors, probably depends on the signal variance as well as its magnitude. Comparison with values from a Monitor Lab 9300 data logger, used at the site since 1979, suggests that the total system errors are dominated roughly 90% by the sensor performance.

TABLE 1. Instrument specifications for tower sensors.

Sensor	Component accuracy
Wind speed	±0.2 m s^{-1} or 1%, whichever is greater Starting speed 0.3 m s^{-1}
Wind direction, including σ_θ	±5.4 degrees Starting threshold 0.3 m s^{-1}
Honeywell dew point	±1°C at or above 11% relative humidity
Cambridge dew point	±0.3°C above a dew point of −30°C
Solar radiation	±27 W m^{-2}
Differential temperature	±0.1°C
Ambient temperature	±0.3°C

In this context, it is apparent that in the long run, routine maintenance such as checking of aspirators, and cleaning of the pyranometer dome, and close monitoring of the system to detect component malfunctions may be more crucial than normal sensor or processor errors.

The tower at the Shearon-Harris Nuclear Plant (SHNP) is located at 35°39'N, 78°57'W (87 m MSL) in a cleared area atop a low hill surrounded by forested, rolling terrain as shown in Fig. 1. Within a 1-km radius, the maximum terrain relief is roughly 20 m. At about 8 km from the tower, the general elevation and relief increase so that the hilltops, extending roughly 50 m higher than the tower base, form the ill defined rim of a broad basin. In the immediate vicinity of the tower, all vegetation except grass is cleared to a radius of at least 100 m. At about 150 m, trees extend to 25 m in height. Since these trees are closer to the tower than ten times their height they probably affect the standard deviation of wind direction measured at the lower wind sensor. However, the rolling terrain and the presence of cleared areas, as, for example, the cleared construction site for the Shearon-Harris Nuclear Plant, located 1 km southwest of the tower, combine to make the site reasonably representative of most of the surrounding region.

The tower at the Robinson Nuclear Plant (RNP) is located at 34°24'N, 80°09'W, 68 m MSL on a flat section of lake shore near the southwest end of Lake Robinson. The lake is roughly 1 km wide and extends 8 km north–south between mostly wooded hills whose tops reach 50 to 60 m above lake level and are located within 2 to 3 km of the shore, as illustrated in Fig. 2. Again although at the SHNP site the tower is in a cleared area, some influence from nearby vegetation is possible at the lower sensor level. Water temperatures were measured monthly along several transects of Lake Robinson. Along a transect adjacent to the tower, temperatures were measured at 1-m intervals from the surface to a depth of 6 m.

3. Data selection and editing

The local sunrise time was rounded to the nearest clock quarter and the 15-min average for tower measurements ending at that time was assigned to time $t = 0$. Thus, the data assigned to $t = 0$ represent a 15-min average for tower measurements ending within ±7.5 min of sunrise. Data from $t = -3$ to $t = 5$ h were then selected for each day to form the dataset used in this study.

Since we are interested in examining trends leading to the formation of the daytime mixed layer, a stringent editing procedure was implemented. If any single variable such as solar radiation, temperature, temperature difference, wind speed, or direction, was missing or in obvious error for any 15-min average for the 8-h period, then all data from that day were omitted.

Obvious errors included occasional solar radiation values greater than the amount incident at the top of the atmosphere at a given time. These were easily isolated from statistics of the 15-min averages combined for each season. A second obvious error involved σ_θ. Occasionally σ_θ was logged as 0.0 when the value was in fact missing. All standard deviations of 0.0 which occurred when a 15-min average wind speed at that level was greater than zero were considered erroneous and dropped from the dataset.

Finally, frequency distributions of σ_θ were examined for anomalies. The appearance of a pronounced 6 to 10° secondary maximum was noted at RNP for all lapse rates, wind directions and speeds during two well-defined periods: 1 January–5 October 1976 and 16 September 1979–1 August 1981. After a likely cause of the anomaly was traced to the signal processor, data obtained during these periods at RNP were omitted from discussion of σ_θ at that site.

During most of the seven-year period, the outputs of the lower Cambridge dew point sensor and the lithium chloride sensor were significantly different. Thus, uncertainties regarding the actual dew point were larger than implied by Table 1. The lithium chloride measurement was almost invariably lower, averaging 1.0°C less, but occasionally reaching 3° to 5°C less during periods when the dew point was near or below 0°C. Furthermore, the Cambridge sensors occasionally experienced large oscillations in output due to sensor malfunctions. But although the dew point information is of limited accuracy, all measured values were retained in the dataset.

Finally, for discussion of the evolution of the wind structure accompanying sunrise, it is important that the effect of the tower structure on the wind measurements in the tower wake be assessed. A site survey at SHNP showed that from the wind sensor position, the tower structure occupied an angle subtended by 304° to 327° from north. According to wind-tunnel studies of a similar open, equilateral tower structure by Gill (1967), the width of the downwind wake at the sensor position is approximately $1.5D$ where D is the length of the side of the tower. Thus, from the sensor location, ambient winds from 295° to 339° may be contaminated by the tower.

However, reductions in wind speed of a maximum of only 0.5 to 1 m s^{-1} during the day and unperturbed frequency distributions of σ_θ for affected wind directions indicate that tower effects are small compared with natural variability and measurement accuracy. Consequently, all wind directions are represented in the results.

4. Results

Throughout this report, the temperature difference (ΔT) between 11 and 60 m serves as an indicator of the strength of the predawn inversion and traces its transition to neutral or superadiabatic conditions after sunrise. The terms "inversion strength" and "neutral" or "superadiabatic" refer only to the 11 to 60 m layer.

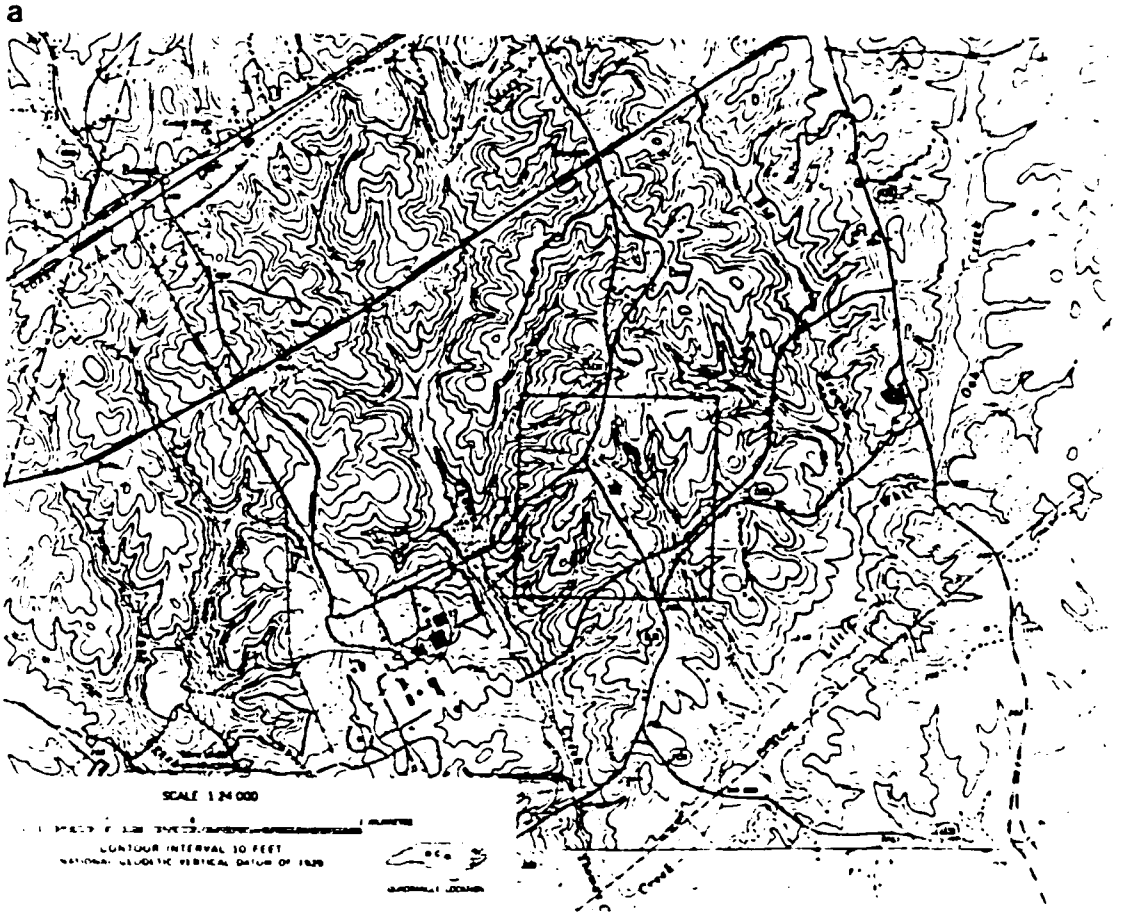

FIG. 1 (a) Topographic contour map showing the location of the micrometeorological tower at the Shearon-Harris Nuclear Plant site; (b) aerial photograph of the tower surroundings. The tower is located at TT.

Predawn inversions, as described by the vertical temperature difference (ΔT) averaged for 1 h preceding local sunrise, are much stronger and more frequent at SHNP. Here, inversions characterize over 70% of all mornings, while neutral and superadiabatic conditions before sunrise are rare, and comprise less than 5% of the sample. Strong inversions, where ΔT is greater than 2.5°C comprise a surprising 30% of the sample days. Results are illustrated in Fig. 3.

Lake Robinson is nearly always warmer than the air at sunrise. For example, on 99.7% of the 595 mornings when winds at 61 m were directed from the lake, the water temperature near the surface was warmer than the 60 m air temperature. This nocturnal heat source apparently affects the microclimate since neutral and lapse conditions are more prevalent and strong inversions less frequent than at SHNP. When the data are grouped by wind directions, in this case 61 m winds from 170° to 350° (directed from land) and from 350° to 170° (directed from Lake Robinson), the lake influence is clearer, as shown in Fig. 4. For a true comparison, the SHNP data are also grouped by the same wind direction criteria. The lake produces a large increase in nocturnal near-neutral conditions, but surprisingly is not associated with many cases of ΔT less than −0.5°C beyond those apparently inherent with synoptic-scale easterly winds. There are some differences between the two sites for land winds also. Again Lake Robinson may be the cause, for at RNP inversions tend to be weaker even though the site is located in a valley.

Since the lake seems to influence the microclimate at RNP, the site will, where possible, be treated as having two regimes, one characterized by winds from the lake and the other by winds from the land. It should be noted, however, that the effects of the lake cannot be totally isolated and probably influence the land regime to some extent also.

Although we have seen a general difference in the inversion climatology at both sites, spatial comparisons can be used to assess similarities, perhaps governed by the synoptic pattern. There is some agreement between frequency of predawn inversions at the SHNP tower and the nearest radiosonde site, located approximately

FIG. 1. (*Continued*)

120 km to the west-northwest near Greensboro, North Carolina. Hosler (1961) presents results of an extensive survey of surface and near-surface based inversion frequency at radiosonde sites in the United States and indicates that for a 3-year period starting in June 1957, low level inversions were measured at Greensboro at 0300 GMT on between 70 and 80% of the days in the sample. Data at 1200 GMT, closer to the predawn conditions studied, here, were characterized by inversions 70% of the time.

Day-to-day correlation of $\overline{\Delta T}$ at RNP and SHNP is 0.75, indicating an underlying synoptic-scale control of the conditions favorable to inversion development at the two rather dissimilar sites. Interestingly, however, the correlation between the two tower sites and Greensboro was low—only 0.49 for SHNP and 0.43 for RNP even though the site-to-site distances are similar. In this comparison, only days for which the radiosonde launch occurred before sunrise were included. The temperature at the surface and first reporting level were combined to give the lapse rate in °C per 100 m. However, generally the first reporting level was above 125 m while the data suggest that most inversions are less than 200 m deep. Thus, it is quite likely that it is the coarse vertical sampling by the radiosonde which results in the low correlation.

So far we have begun to characterize the predawn inversion strength near the ground for a long time period at two sites of differing microclimate. Let us now describe the seasonal frequency of strong versus weak inversions and trace the morning transition to superadiabatic conditions at each site. Since synoptic-scale factors are likely to be important in creating conditions governing inversion development, we might expect similarities in seasonal frequency of strong inversions at both sites. However, because of the local influence of the lake at RNP, we might expect differences in the transition process for lake versus land winds or from one site to the other.

Some effort was expended to detect any natural stratification of $\overline{\Delta T}$, and for that matter, all the observed variables for the predawn hours each day. The procedures used in this detection effort include the Wolfe (1970) NORMIX program which uses maximum-likelihood techniques to identify mixtures of multivariate normal distributions, Ward's grouping method and the average linkage procedure (see Anderberg, 1973), both of which are hierarchical clustering algorithms. How-

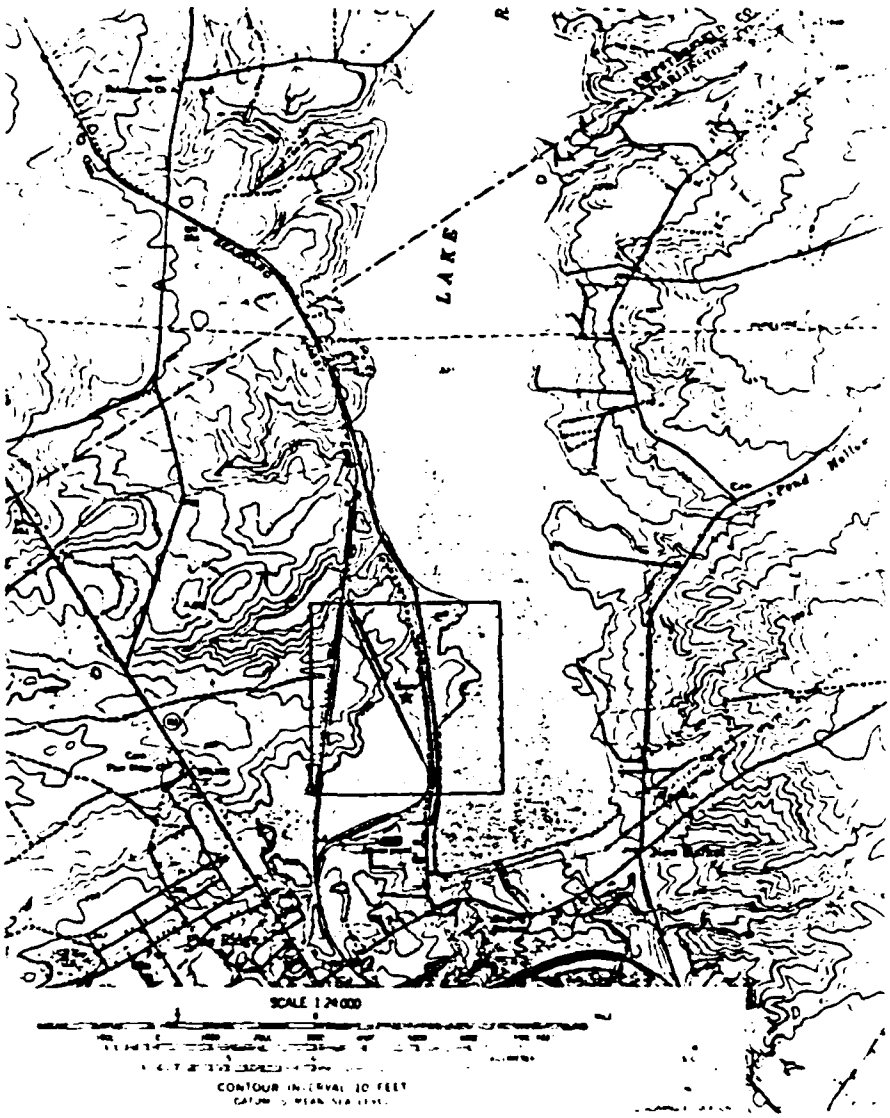

FIG. 2. Topographic contour map showing the location of the micrometeorological tower at the Robinson Nuclear Plant site.

ever, none of the three techniques provided evidence for natural groupings for any of the observed variables. Rather, each was characterized by a continuous spectrum of values over its entire range. Without natural grouping, days are simply ranked by $\overline{\Delta T}$ and arbitrarily divided into nine classes as defined in Table 2. Also given in Table 2, for reference at SHNP, are the Brunt-Väisälä frequencies defined as

$$N = \left(\frac{g}{\bar{T}}\frac{\overline{\Delta\theta}}{\Delta z}\right)^{1/2}$$

where g is the acceleration of gravity, and $\bar{T}$ and $\overline{\Delta\theta}$ refer to the class-averaged absolute temperature and vertical difference in potential temperature, respectively, for the hour preceeding sunrise.

First, the frequency of each $\overline{\Delta T}$ class can be compared for each month as illustrated in Fig. 5 for SHNP. Near-neutral conditions (classes 1 and 2) are most frequent beginning in fall and extending through winter. This is not surprising since synoptic-scale disturbances frequent during these months are often accompanied by overcast or windy conditions unfavorable for the development of nocturnal inversions. It is also interesting to note from Fig. 5 that at SHNP weak $\overline{\Delta T}$ categories (classes 4 through 6) are most frequent in summer, but strong categories (classes 8 and 9) are not. They have a marked preference for fall and early spring and are relatively rare in summer. Similar results are found at RNP.

The absence of strong inversions in summer at both Carolina sites is in marked contrast with results from

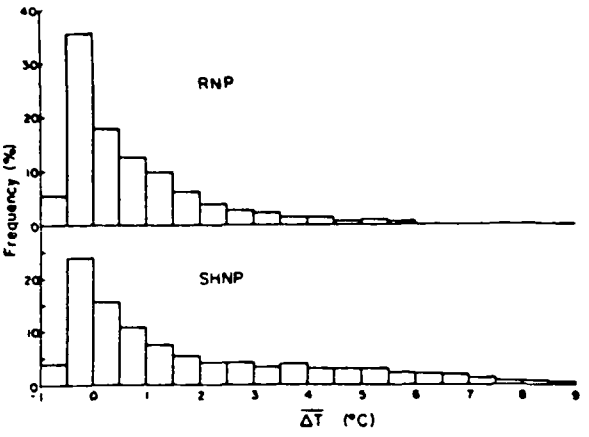

FIG. 3. The inversion strength expressed as the temperature difference (°C) from 60 to 11 m averaged for the hour preceding sunrise, 1976–82, for the Robinson (RNP) and Shearon-Harris (SHNP) sites.

rural Ames, Iowa (Takle et al. 1976) and Argonne National Laboratories (Moses and Bogner, 1967) which show that the strongest inversions occur in summer. Even considering the differences in monitoring levels among the sites (for example, 2 to 32 m at Ames versus 11 to 60 m for ΔT in this study) the seasonal preferences are significantly different. We cannot totally rule out local topography as a factor, since advective effects of terrain or even episodic gravity wave events may have a seasonal preference. However, one factor which RNP and SHNP sites share and the other sites do not is abundant water vapor in the boundary layer. Mixing ratios at or above 15 g kg^{-1} are common throughout the southeast in summer. Despite light winds and cloudless skies, such abundant moisture is likely to drastically reduce the net radiative loss at night and curtail surface inversion development. It would be interesting to investigate if and how water vapor becomes a limiting factor in inversion development.

Hodographs of wind frequency at both sites (Fig. 6) show a preference for a bimodal distribution of wind directions of north or northeast and southwest. This distribution has been documented in climatological summaries for the Carolina piedmont (*Climatic Atlas of the United States, 1968*) and is largely due to synoptic-scale influence. High frequencies of northeast winds are most closely associated with near-neutral conditions and probable cloudiness accompanying east coast cyclone or frontal activity. At both sites there is strong continuity of wind direction both with height and time during morning transition for this near-neutral class.

For stronger inversion days, however, large differences emerge. At sunrise when the inversion is well established, the hodographs differ so markedly with height that the differences with height are greater than those from one site to the other. The 12 m winds, commonly from the northwest, especially at SHNP, appear unrelated to those at 61 m. A reference to Fig. 1a shows that if such frequent winds are associated with density flow, as would be expected during strong inversions, the topographic control may be quite subtle. As the well mixed daytime conditions are established, the northwest wind preference disappears and at both sites the hodographs for the upper and lower levels are similar.

Finally, there is some evidence of a lake wind oscillation at RNP, where for mornings with moderate and strong inversions, offshore winds (from the west) are more frequent at both levels at dawn while onshore winds (from the east) are more frequent during the day. This oscillation is most apparent for strong inversion days when, as will be shown later, solar radiation is most intense. The presence of a lake breeze circulation is certainly not surprising for a lake this size and such circulation may help explain why nocturnal

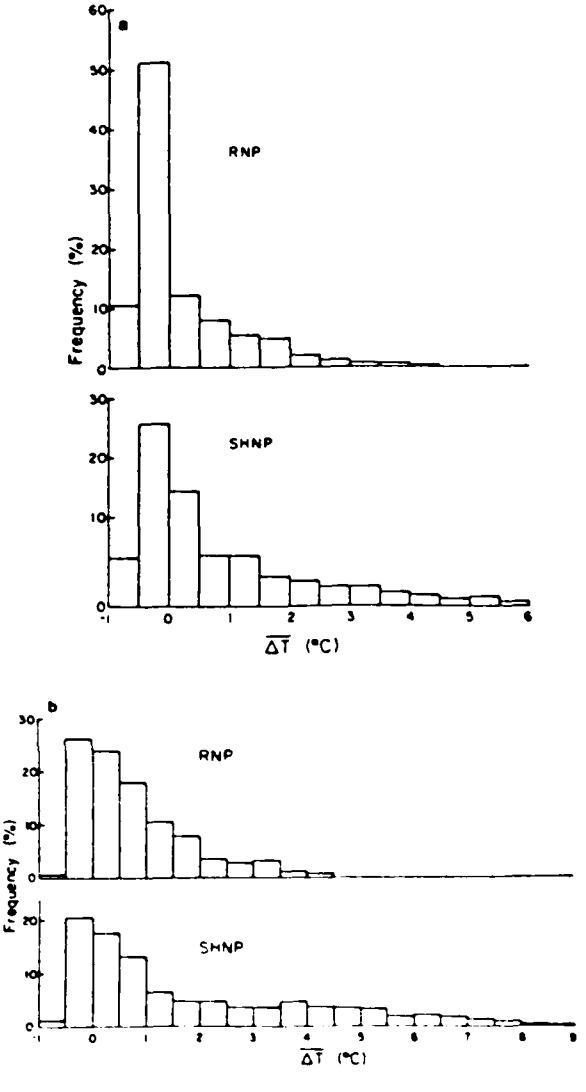

FIG. 4. As in Fig. 3 for (a) easterly winds (from the lake at RNP), (b) westerly winds.

TABLE 2. Definitions and distribution of predawn ΔT classes (1976–82).

Class	Predawn average 11 to 60 m temperature difference, $\overline{\Delta T}$ (°C)	N	Number of days (%)			
			SHNP	RNP		
				All winds	Land winds	Lake winds
1	$-0.75 \leq \overline{\Delta T} < -0.25$	7.5	216 (16)	436 (23)	65 (11)	264 (44)
2	$-0.25 \leq \overline{\Delta T} < 0.00$	15.7	148 (11)	309 (13)	100 (16)	102 (17)
3	$0.00 \leq \overline{\Delta T} < 0.25$	20.5	108 (8)	196 (10)	84 (14)	46 (8)
4	$0.25 \leq \overline{\Delta T} < 0.75$	25.9	170 (13)	272 (15)	119 (19)	55 (9)
5	$0.75 \leq \overline{\Delta T} < 1.50$	32.9	172 (13)	288 (15)	110 (18)	54 (9)
6	$1.50 \leq \overline{\Delta T} < 2.50$	41.6	122 (9)	187 (10)	72 (12)	44 (7)
7	$2.50 \leq \overline{\Delta T} < 4.00$	51.3	145 (11)	117 (6)	46 (7)	19 (3)
8	$4.00 \leq \overline{\Delta T} < 6.00$	62.5	147 (11)	59 (3)	19 (3)	9 (2)
9	$6.00 \leq \overline{\Delta T}$	74.5	89 (7)	7 (*)	2 (*)	2 (*)
	Total number of days		1317	1817	617	595

Note: N is the Brunt-Väisälä frequency $\times 10^{-3}$ s^{-1} corresponding to the average class statistics at SHNP.
* Less than 1%.

inversions at RNP are generally weaker than those at SHNP even during west winds.

Turning now from a general climatological site description to an analysis of the development of the daytime mixed-layer, let us examine the detailed changes in measured quantities during the morning transition. Even when all seasons and days with varying cloud amounts are combined to represent average conditions, the results reveal a remarkably logical and well-ordered transition from stable nighttime conditions to the well-mixed surface layer characteristic of the daytime. Strong predawn inversions tend to persist longer even though low-level heating begins sooner, as illustrated for SHNP in Fig. 7. By contrast, for weaker inversions warming is less dramatic and begins more nearly simultaneously at both levels. It is noteworthy that the cumulative solar radiation, ΣG, is greatest on mornings with strongest predawn inversions as illustrated in Fig. 8. A nonparametric test using Wilcoxon scores indicates that the differences in ΣG are significant among all inversion classes even as early as 2 h after sunrise. This is not surprising since inversions develop most readily under cloudless conditions which generally persist after sunrise.

As the inversion breaks down, changes in surface-layer structure can be interpreted physically. Again, these changes are most dramatic for days with the strongest predawn inversions, as illustrated for class 9 in Fig. 9, for example. The 11 m temperature stops its gradual downward drift and begins warming as early as 30 to 45 min after sunrise. This is in response to very small amounts of local insolation. The distant stand of deciduous forest toward the east delays local sunrise at the tower base by roughly 20 to 25 minutes, although during winter, vegetation is less dense and the delay is reduced. Thus, it is probably advection of warmer air from nearby sunlit surfaces that produces the slight warming at 11 m during the first half hour.

Soon after measurable warming occurs, the standard deviation of the wind direction at 12 m begins to increase. The effect, smoothed in Fig. 9 by averaging 15-min sequences over 89 d, is, in fact, produced by the increased frequency of short turbulent bursts which for this class appear to begin about 1½ h after sunrise.

The warming at 11 m is apparently confined within the tower layer (i.e., between 11 and 60 m) for almost 1½ h. It is not until about 2 h after sunrise that the slow cooling and uniformly low σ_θ values at 60 m are interrupted. At about 2 h after sunrise, however, mixing begins to reach the upper level, warming begins, and the wind speed drops as momentum is exchanged with lower layers. By about $t = 3$ h, lapse conditions are reached, the tower layer is fully coupled, and the 60 m wind is starting to increase as lost momentum is replaced from progressively higher levels. In most respects the trends of wind speed at both levels closely resemble those obtained during the Wangara experiment and at Riso, Denmark, as illustrated by Mahrt (1981).

The trend curves for σ_θ, shown in Fig. 9 represent only average values. Full frequency distributions of σ_θ at 11 m before and after transition are illustrated in Fig. 10. To present smooth representative curves, ΔT classes 5 through 9 are combined. Predawn conditions are represented by combining all 15 min average σ_θ values in these classes for 3 h before sunrise. Likewise, conditions after transition are represented by all σ_θ values for 3 to 5 h after sunrise. Other than an obvious shift to the right by about 10°, the frequency distribution of σ_θ is remarkably similar for day versus night. Further partitioning of classes by wind speed or a bulk stability parameter might yield different results.

When the transition at RNP is compared with that already described for SHNP, differences are surprisingly small. Figures 11a and 11b compare trends at the two sites for similar wind groups. For this comparison, classes 7 through 9 are combined. At SHNP this combined class was reduced from numbers given in Table 2 so that ΔT at sunrise is comparable with that at RNP.

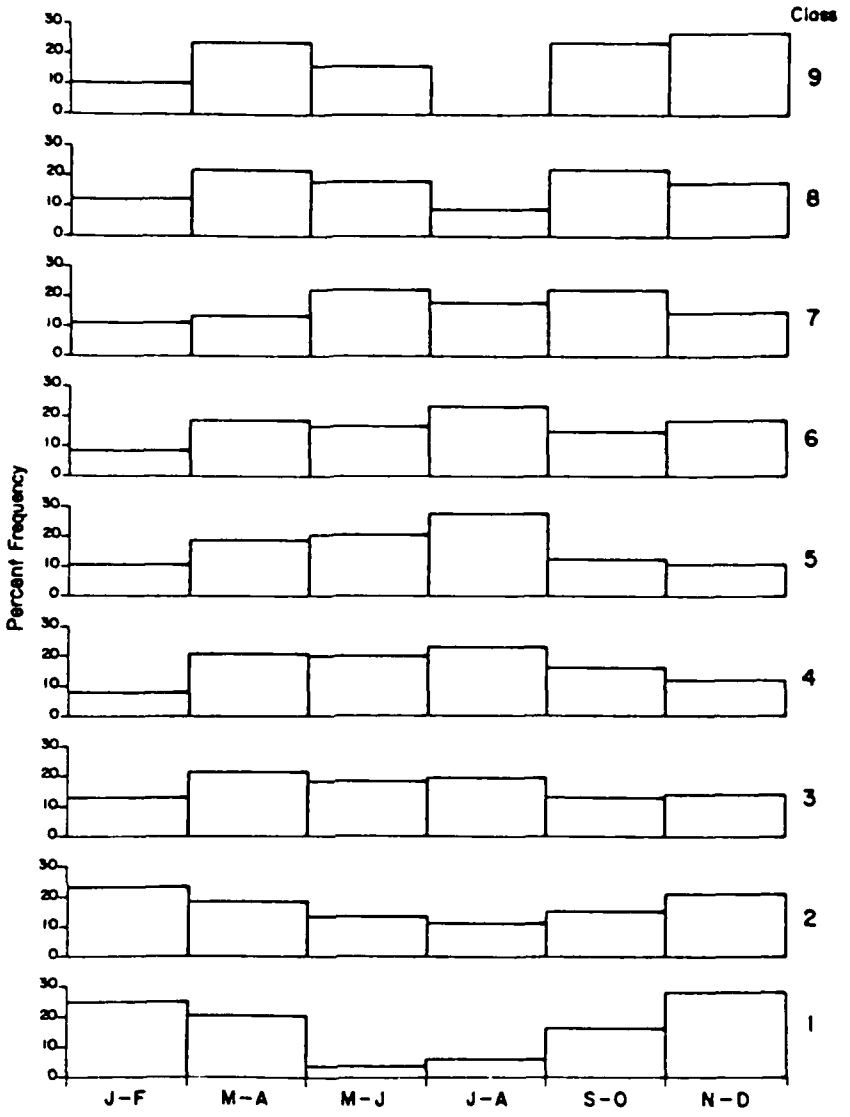

FIG. 5. Seasonal distribution of the inversion classes listed in Table 2 for SHNP. Weak inversions are included in classes 3 through 5 while strong inversions occur in classes 7 through 9.

There is some difference in the rate of change, but by and large, ΔT curves are similar at both sites. However, there are a few important differences. For lake winds at RNP, ΔT decreases to -0.5°C (corresponding to the dry adiabatic lapse rate for the 50 m layer) more slowly, no doubt because of advection of relatively stable air from the lake. From the Wilcoxon method, differences in ΔT become significant at the 95% confidence level by 2 h after sunrise. Significant differences in ΔT for 1 and 2 h after sunrise are also found for mornings with land winds. Here, the ΔT decrease is initially more rapid at RNP, probably because solar radiation is significantly greater.

By far the largest effect of Lake Robinson is in promoting vertical momentum exchange during the night. This is seen in Fig. 11b when wind speeds for lake wind conditions at RNP are compared to any of the other three groups. Wind shear during predawn hours is suppressed for this group and the morning transition is therefore less dramatic. The reduced shear is consistent with upward eddy heat flux and associated momentum exchange over the warm lake surface.

It is also interesting to contrast the σ_θ trends for the two sites and wind conditions, as illustrated in Fig. 12. Here we see that although there are expected differences in transition for lake versus land winds, the predawn turbulence for lake winds certainly does not resemble daytime intensity. For these winds the tower is situated in a wake region where the perturbed mean flow and turbulence fields are beginning to recover to values

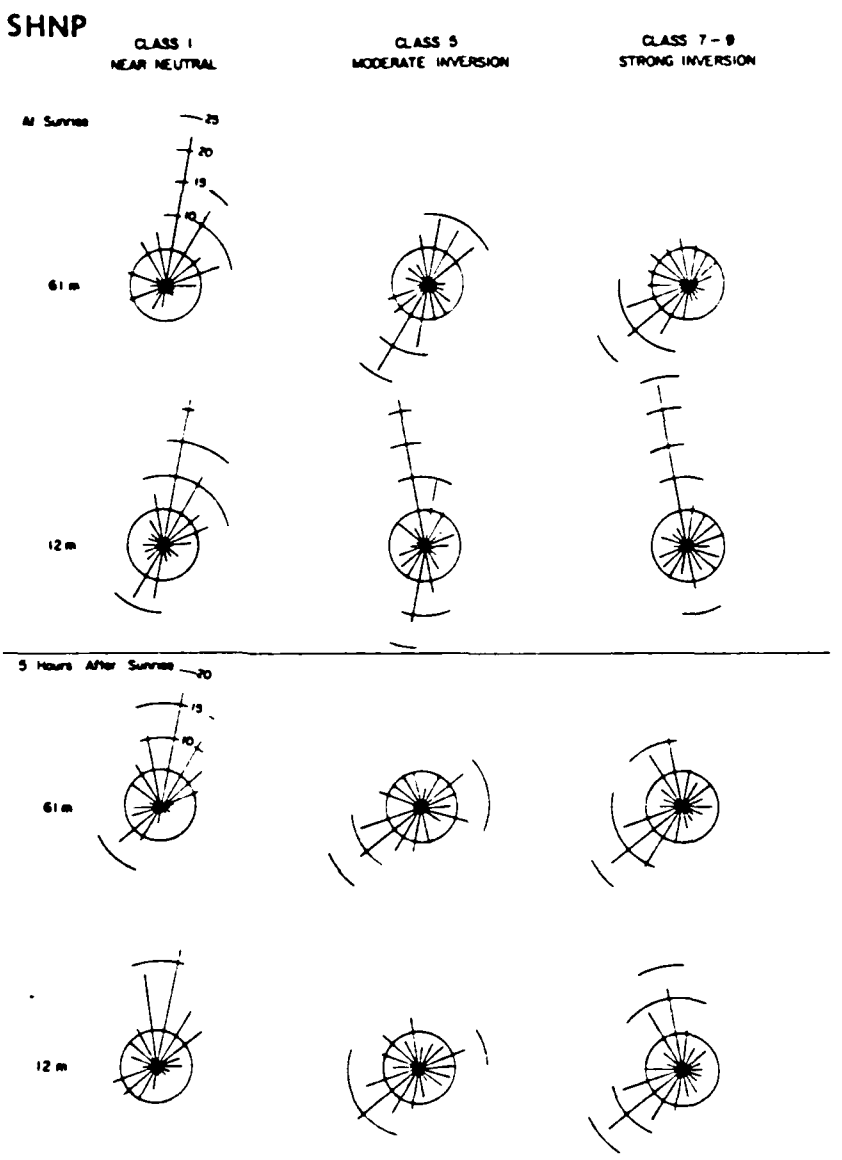

FIG. 6. Wind frequency hodographs before and after the morning transition for both tower levels. Three $\Delta\bar{T}$ classes are illustrated for both sites.

characteristic of the nocturnal inversion over land. Note that σ_θ at 61 m before dawn is greater for lake winds than for any other group.

The whole process from sunrise to establishment of lapse conditions in the tower layer at both sites takes about 3 h for classes 7 through 9. Inspection of Fig. 7 reveals that for SHNP the average time varies from 2.2 to 3 h depending on $\Delta\bar{T}$.

This average transition time is much longer than that deduced from a study of inversion transition at a rural site near St. Louis (Godowitch et al., 1979). The latter, for which detailed measurements were available for 52 summer mornings, documented the growth of the mixing height to 100 m by 1½ to 2 h after sunrise. Also, in the Ames, Iowa study by Takle (1983) and Takle et al. (1976) it was found that on clear mornings 1–2 h were required from sunrise to establishment of unstable conditions through a 32 m layer.

At first glance, the difference at Ames versus the Carolinas might be attributed to the difference in tower height, since the towers at both RNP and SHNP are nearly twice as high as at Ames. However, Takle et al. (1976) state that there is little difference in the transition time for any tower interval based at 2 m. The difference among sites may, nevertheless, be largely due to sampling differences. For example, if a shallow superadi-

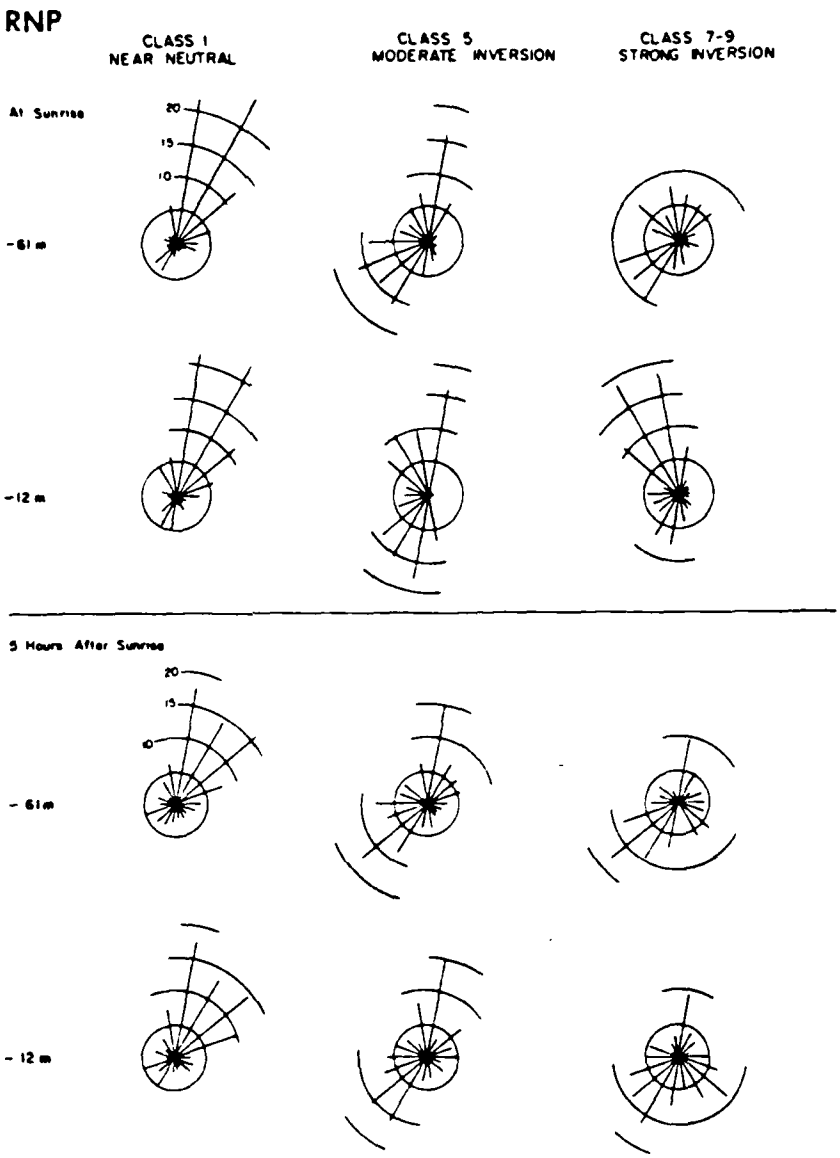

FIG. 6. (*Continued*)

abatic layer becomes established at the surface during the morning, then the placement of the lowest temperature sensor may critically determine the apparent onset of neutral conditions as monitored through a coarse vertical sampling interval. Thus, apart from true site differences, it may be that the location of the lowest sensor produces the climatological differences. With a sensor at 2 m at Ames we would expect a more rapid apparent transition than at SHNP or RNP where the lowest sensor is at 11 m.

In closer agreement with our result, the Brookhaven data, representing two years of measurements over flat terrain, show that superadiabatic conditions become established in the lowest 60 m at about 4 h after sunrise under average cloudiness (Singer and Raynor, 1957). The lowest temperature sensor at Brookhaven was at 11 m.

The differences among these studies may also stem from differences in choice of variables used to describe the state of the transition. For example, in our case with only two measurement levels, the mixing height may be very close to the upper level when both sensors measure the same temperature. If this "isothermal" state is used to indicate the end of the morning transition for the tower layer, the transition time is greatly reduced. Figures 13a, b illustrate the distribution of the latter transition time for both sites.

On the other hand, if turbulence is selected as the

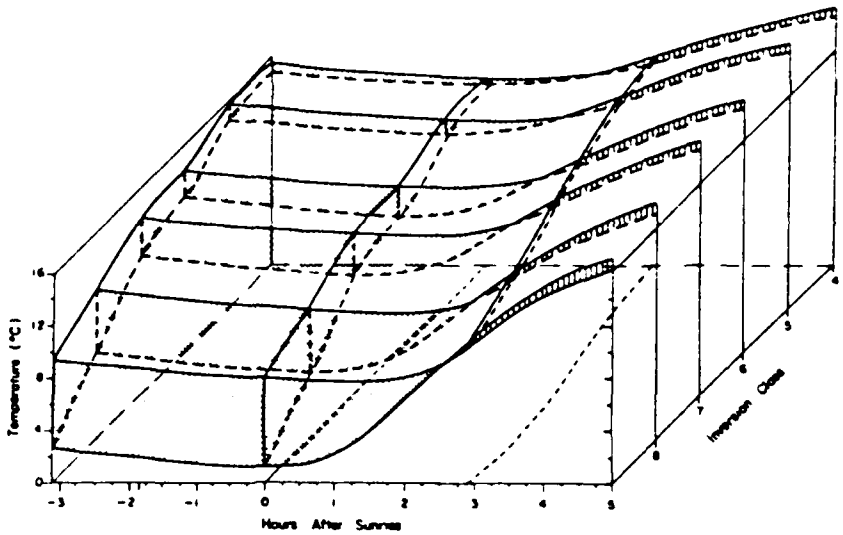

FIG. 7. Class-average temperature trends during the morning transition for SHNP, 1976–82. Both tower levels are included for each class. Dot shading indicates the presence of the inversion, while line stippling indicates a superadiabatic lapse rate in the tower layer.

variable to monitor transition, the longer transition times of 2 to 3 h are obtained. The latter choice is generally most physically meaningful since this is the time it takes for σ_θ to reach its typical daytime value at the 60 m level.

So far we have seen that although there are several important differences in the surface layer at RNP and SHNP, especially at night, by and large, the transition appears to follow an orderly pattern at both sites. The examination of average behavior of large classes based on $\Delta\overline{T}$ before sunrise shows that the transition time is proportional to $\Delta\overline{T}$. This was also found true by Hickle et al. (1976).

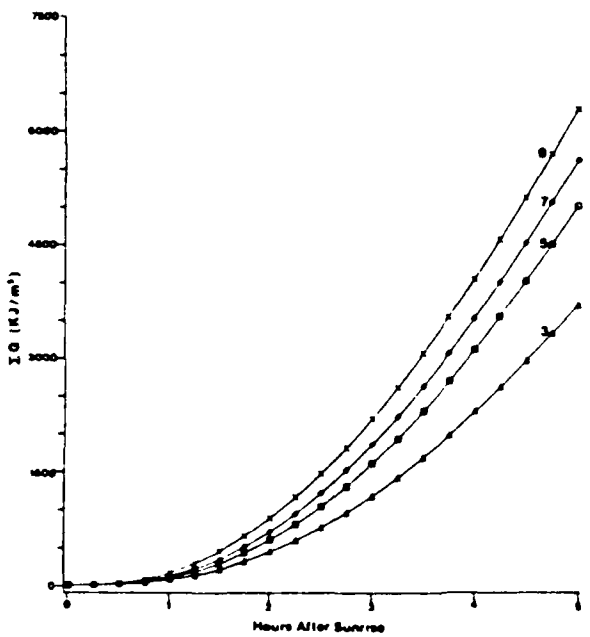

FIG. 8. Cumulative solar radiation incident at SHNP for four selected classes as indicated.

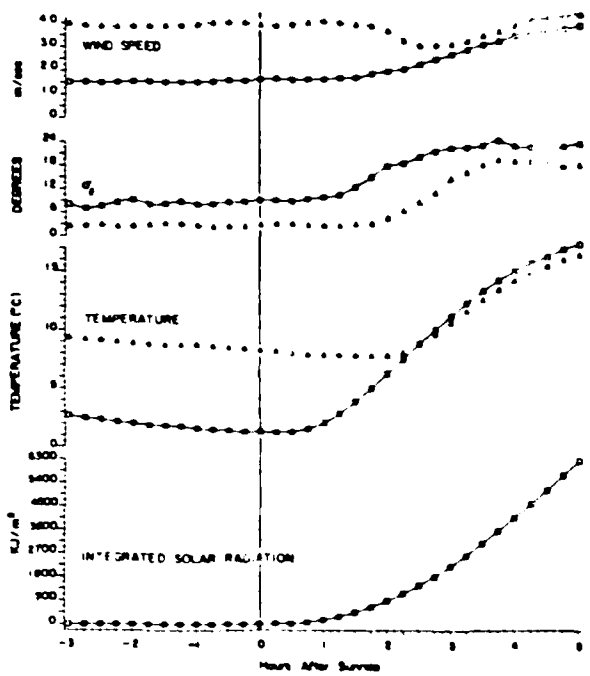

FIG. 9. Mean statistics for class 9 (strongest inversion days) at SHNP. Triangles denote values for the upper tower level, while squares denote those for the lower level.

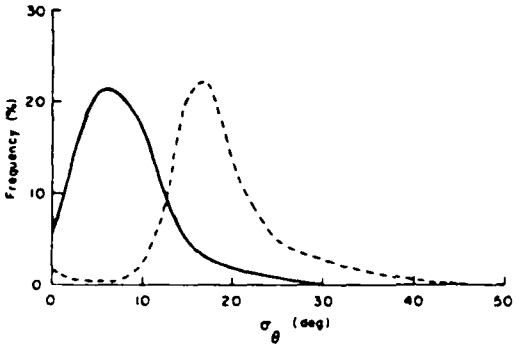

FIG. 10. Frequency distribution of σ_θ at 11 m for $\overline{\Delta T}$ classes 5 through 9 at SHNP. The solid line represents conditions during the 3 h prior to sunrise, while the dashed line represents conditions from 3 to 5 h after sunrise.

The question then arises as to whether other variables, such as wind shear or insolation are significantly related to the morning transition time. Certainly, for example, changes in cloudiness after sunrise ought to have an effect. Also, there is the key question of whether the highly organized transition behavior for class-averaged data implies a reasonable predictability of the time of morning transition on a daily basis. Would such a predictive scheme be similar at both sites? To explore these questions, a regression model was developed and tested at both sites.

Regression models. There are many procedures available for constructing a regression model; Draper and Smith (1981) recommend the stepwise procedure. In the present case, the standard stepwise procedure has been supplemented with the maximum R^2 (coefficient of multiple determination) improvement technique (MAXR) developed by J. Goodnight of the SAS Institute (1982). Goodnight considers this technique superior to the standard stepwise method and nearly as good as the "all-possible" regression approach.

The Goodnight procedure does not attempt to find the single best model; rather, it attempts to find the best one-variable, two-variable, etc., model. Initially, MAXR finds the one-variable model yielding the highest R^2. The next variable to enter the model is the one that provides the greatest increase in R^2. With the two-variable model in hand, each variable included in this model is compared with each variable which is not in the model. Each time a comparison is made, MAXR ascertains if removing one variable and substituting another in its place will increase R^2. Once all possible replacements have been considered, the one that yields the greatest increase in R^2 is made. This procedure continues until the best two-variable model has been identified. At this point no variable switch would increase R^2; MAXR then moves on to the best three-variable model.

The modeler is ultimately faced with the task of having to select a final model from among the best one-,

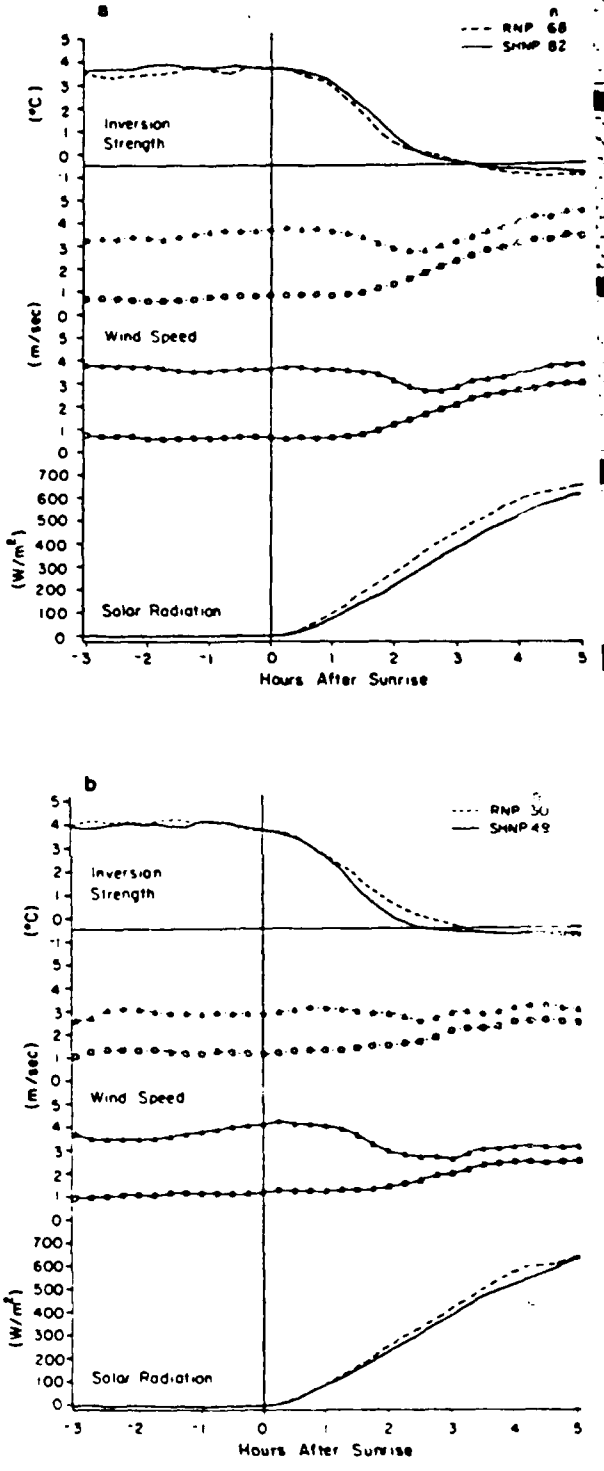

FIG. 11. Comparison of the morning transition for RNP (dashed) and SHNP (solid) for days with similar predawn inversions. Included for comparison: vertical temperature difference, with lapse conditions indicated by the horizontal line; wind speed at the upper (triangles) and lower (squares) levels; and solar radiation for (a) west winds and (b) east winds. In each case n indicates the number of days in the sample.

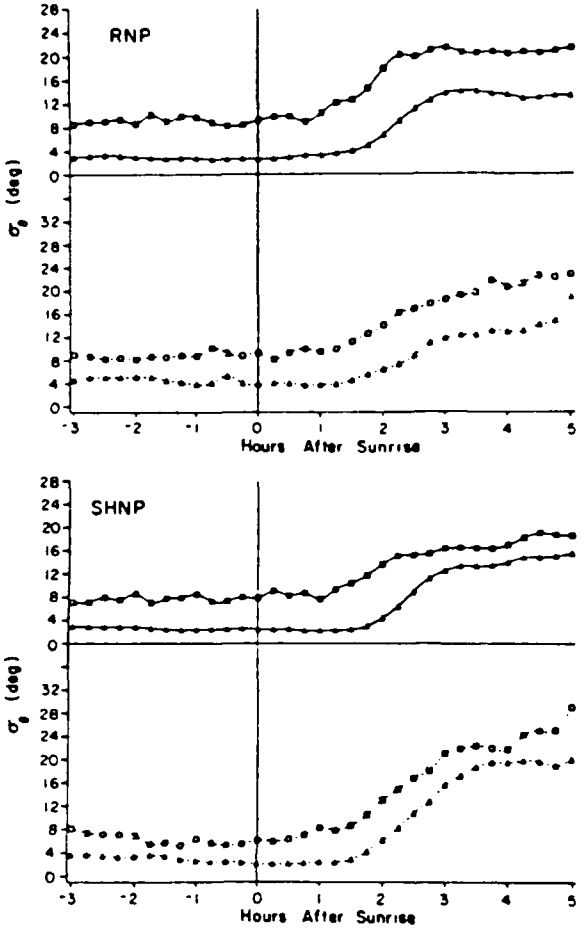

FIG. 12. Standard deviation of wind direction (σ_θ) for the same inversions as in Fig. 11. Solid lines are trends during west winds and dashed lines are those for east winds.

two-, etc., variable models provided by MAXR. In the present case, the model selected had the least number of independent variables while maintaining a high R^2 value.

Preliminary results of the regression models highlighted the importance of ΔT as a predictor of inversion breakdown, but its predictability was reduced by variations in cloudiness after sunrise. Thus, it seems reasonable to partition the data into clear and nonclear mornings, examine their prior and conditional probabilities, and model each separately.

The following procedure was used to define and identify clear mornings:

1) for times when the extra-atmospheric irradiance EI, defined as the total solar radiation incident on a horizontal surface at the top of the atmosphere, is greater than or equal to 300 W m^{-2}, the following must be true for every 15-min average

$$G^* \geq 0.213 \ln(EI) - 0.813 \quad (1)$$

where $G^* = G/EI$; and

2) For the 15-min interval i,

$$G_i^* \geq G_i^* - 0.05G_{i-1}^*. \quad (2)$$

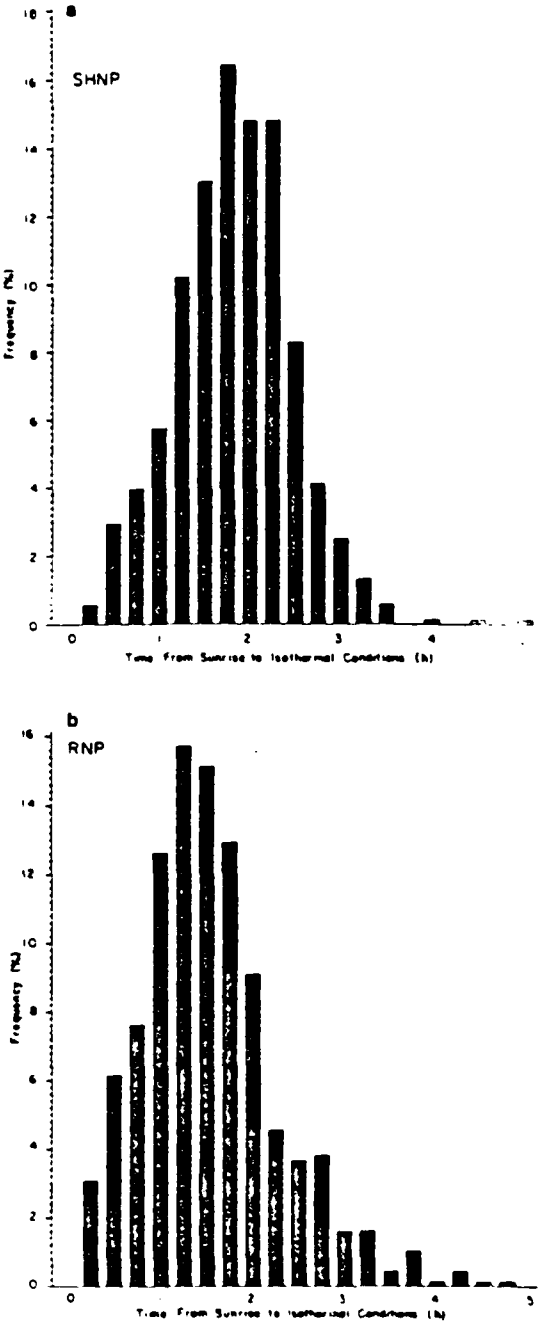

FIG. 13. Distribution of the time from sunrise until both upper and lower temperatures are equal for all modeled days at (a) SHNP and (b) RNP

TABLE 3. Clear day probabilities.

	Annual		Winter/spring		Summer/fall	
Probability	RNP	SHNP	RNP	SHNP	RNP	SHNP
$P(3/1.5)^*$	0.47	0.35	0.52	0.33	0.39	0.42
$P(2/2.5)$	0.70	0.70	0.77	0.69	0.60	0.70
$P(1/3.5)$	0.80	0.83	0.88	0.85	0.68	0.79
$P(3/1.5)^{**}$	0.53	0.65	0.48	0.67	0.61	0.58
$P(2/2.5)$	0.30	0.30	0.23	0.31	0.40	0.30
$P(1/3.5)$	0.20	0.17	0.12	0.15	0.32	0.21

* Conditional probability of 3 more clear hours given that the first 1.5 h after sunrise were clear, etc.

** Conditional probability of at least one of the next 3 hours being nonclear given that the first 1.5 hours after sunrise were clear, etc.

If both criteria 1 and 2 were met for all 15-min averages for the 4 h after sunrise, the day was designated as clear. Equation (1) was empirically derived from frequency distributions of G^* over varying EI intervals for a large number of days at both sites. As EI increases, the highest values of G^* form a discernible, sharpening peak in the frequency distribution. This peak represents clear sky conditions, while the background of noisier, lower G^* values represents nonclear conditions. Equation (2) represents the lower-bound in the G^* peak.

Tables 3 and 4 contain the clear and nonclear-day empirical probabilities for the first 4.5 h after sunrise at both power plants. Nonclear conditions dominate the probabilities at the two sites on both an annual and seasonal basis. Even when the first 1.5 h have been clear, the conditional probability that the next 3 h will be clear is generally less than 0.5. When the first 1.5 h have been nonclear, the conditional probability that nonclear conditions will prevail until the end of the period is generally above 70%.

Regression models were developed for Robinson Nuclear Plant and Shearon-Harris Nuclear Plant for clear and nonclear days. The dependent variable in each of the four models was t_B, the time from local sunrise until the temperature at both 11 and 60 m was the same. Thus, based on the previous discussion, we are modeling a state which marks a stage in the transition which occurs 1 to 2 h before daytime σ_θ values are reached. The best independent variables were $\Delta\overline{T}$ the dew point from the 11 m lithium chloride instrument, $\overline{T_d}$, the wind speed at the upper and lower levels $\overline{V_u}$ and $\overline{V_l}$, respectively, and the component wind shear, $S = (\Delta\bar{u})^2 + (\Delta\bar{v})^2$, where overbars denote a 1-h average ending at sunrise and deltas denote height differences.

The models developed are as follows:

(i) Shearon-Harris Nuclear Plant

Clear day

$$t_B = 0.9253 + 0.1731\Delta\overline{T} + 0.0220\overline{Td}$$

$$R^2 = 0.76$$

$$N = 100$$

Nonclear day

$$t_B = 1.238 + 0.1843\Delta\overline{T} + 0.0160\overline{Td}$$

$$R^2 = 0.31$$

$$N = 675$$

(ii) Robinson Nuclear Plant

Clear day

$$t_B = 1.220 + 0.2350\Delta\overline{T} - 0.0751\overline{V_u}$$

$$R^2 = 0.55$$

$$N = 274$$

Nonclear day

$$t_B = 1.587 + 0.309\Delta\overline{T} - 0.1414\overline{V_u}$$

$$R^2 = 0.42$$

$$N = 681$$

Figures 14a, b illustrate the best and worst case models for comparison.

A careful examination of the residuals for each of the four models gave no indication that these examples were not appropriate and that our modeling assumptions were not valid.

The derived models were designed to be forecast models; consequently, this attribute required testing. The derived models can be used in conjunction with the entire dataset employed in their development to produce forecasts of the dependent variable. The forecast error which arises in this case is an apparent error ($\overline{\text{err}}$) rate (see Efron and Gong, 1983) which is likely to underestimate the true error (err) rate because of the way the forecasts were produced. Table 5 shows the apparent error rates for each of the four models. A

TABLE 4. Nonclear day probabilities.

	Annual		Winter/spring		Summer/fall	
Probability	RNP	SHNP	RNP	SHNP	RNP	SHNP
$P(3/1.5)^*$	0.73	0.78	0.72	0.68	0.74	0.88
$P(2/2.5)$	0.90	0.95	0.91	0.93	0.89	0.96
$P(1/3.5)$	0.94	0.98	0.96	0.97	0.92	0.98
$P(3/1.5)^{**}$	0.27	0.22	0.28	0.32	0.26	0.12
$P(2/2.5)$	0.10	0.05	0.09	0.07	0.11	0.04
$P(1/3.5)$	0.06	0.02	0.04	0.03	0.08	0.02

* Conditional probability of 3 more nonclear hours given that the first 1.5 h after sunrise were nonclear, etc.

** Conditional probability of at least one of the next 3 h being clear given that the first 1.5 h after sunrise were nonclear, etc.

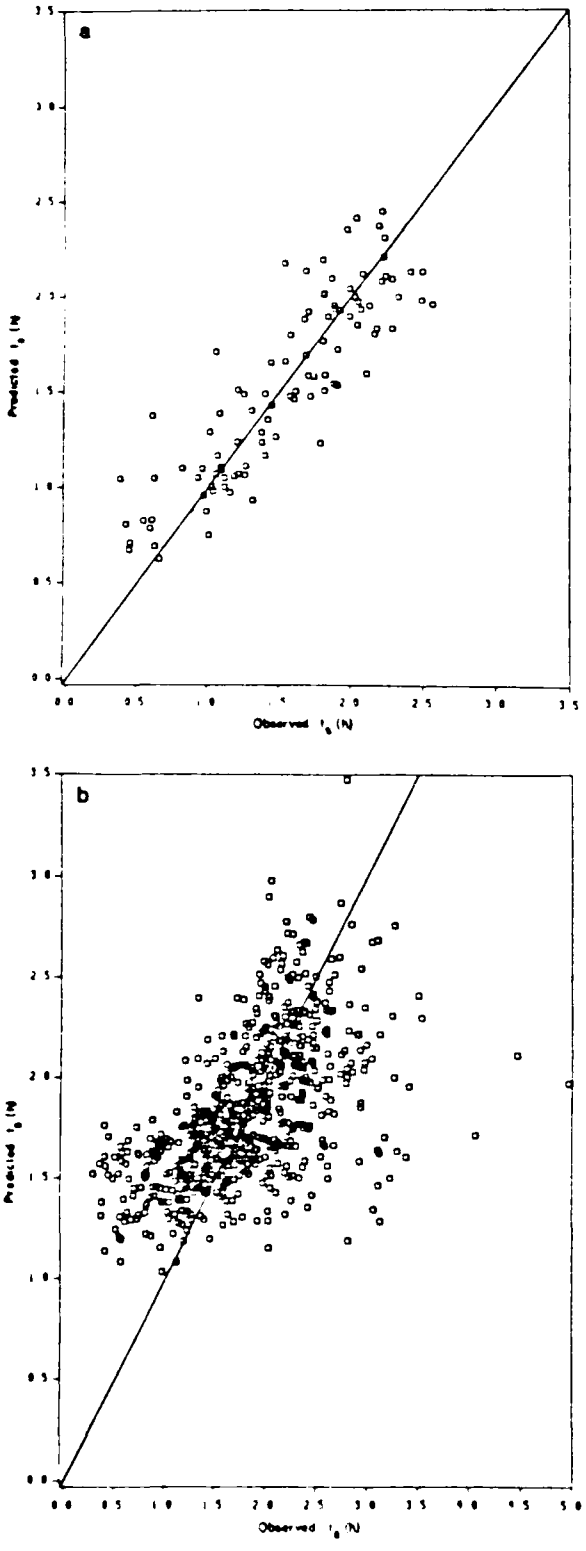

FIG. 14. Model results for SHNP for (a) clear days and (b) nonclear days.

random variable of interest is the overoptimism, which is true error rate minus apparent error rate. The expected overoptimism equals the expected value of the difference (err − $\overline{\text{err}}$). Since the true error rate is unknown, the overoptimism is estimated by subtracting the apparent error rate ($\overline{\text{err}}$) from the cross-validated estimate (err*) of the true error (err). The cross validation estimate of the true error is thus the error rate over the observed dataset, not allowing a certain portion of the data to enter into the construction of the equation to be used for its own prediction.

In the present case, the cross validation estimate was obtained by randomly extracting 10% of the data points from each model, reestimating the model using the stepwise procedure, and then using the reestimated model to forecast t for the 10% sample that was extracted. This procedure was repeated ten times for each of the four datasets. The forecast errors were averaged and appear in Table 5 under the heading "cross-validation estimate." The difference (err* − $\overline{\text{err}}$) is an estimate for the overoptimism given by (err − $\overline{\text{err}}$). It appears in the last column of the Table 5. The results seem to indicate that overoptimism was not a problem and that the apparent error provides a good guide to the way in which the model will perform. See Efron and Gong (1983) for additional comments on the relationship between (err* − $\overline{\text{err}}$), overoptimism, and expected overoptimism. The authors raise a question concerning the ability of (err*) to provide a good estimate of (err).

One interesting test using both models and sites is to determine the error involved in modeling t_B at one site with the model developed for the other site. Such a test quantitatively assesses the effect of local factors on the inversion breakdown. Table 6 documents the results of the model/site intercomparison.

It is of interest to know how both the R^2 and rms error values vary when the models are interchanged. Surprisingly, the clear-day RNP model actually performs better at SHNP than at the site for which it was developed. This result is due to the fact that there is greater variability in both the independent and dependent variables at RNP than at SHNP. Such variability is entirely consistent with results shown previously in which the lake influence was described. To place the

TABLE 5. Model cross-validation error analysis.

Dataset	Apparent error ($\overline{\text{err}}$) (h)	Cross-validation estimate (err*) of (err) (h)	err* − $\overline{\text{err}}$ (h)
RNP (clear)	0.329	0.316	−0.013
RNP (nonclear)	0.567	0.577	+0.010
SHNP (clear)	0.269	0.262	−0.007
SHNP (nonclear)	0.533	0.553	+0.020

TABLE 6. Results of exchanging models.

Base model	Model results: Site predicted	R^2	rms error
		Clear day	
RNP	RNP	0.55	0.33
	SHNP	0.67	0.31
SHNP	SHNP	0.76	0.27
	RNP	0.53	0.34
		Nonclear day	
RNP	RNP	0.42	0.56
	SHNP	0.28	0.55
SHNP	SHNP	0.31	0.53
	RNP	0.36	0.60

modeling in its proper context, however, one should note that for a given site, the model developed for that site gives the best results.

5. Conclusions

The microclimate of the two sites differs in many significant ways. Most of these differences appear to be associated with the presence of Lake Robinson adjacent to the RNP site, rather than to its valley location. For example, the low frequency of strong inversions, especially with winds directed from the lake, tends to dominate the predawn environment. This same wind regime also seems to be characterized by thermally driven mixing from the warm lake surface, since the vertical wind shear is reduced and σ_θ is increased over expected values. The morning transition of the surface layer from the nocturnal inversion to a well-mixed daytime state proceeds somewhat slower than expected at RNP, given similar predawn conditions to those at SHNP. This is somewhat surprising since the radiation intensity at RNP is generally greater.

Despite the differences, there is a great deal of similarity between the climatology of the invesion and its transition at both sites. For example, there is a relatively high correlation (0.71) in the day-to-day value of ΔT in the predawn hour at both sites. The seasonal preference for the strongest inversions to occur in fall and winter, with weaker inversions in summer is nearly identical at both locations.

These similarities illustrate that even among dissimilar sites, inversion frequency is not entirely site specific. Thus, there is encouraging support for the idea that one can spatially extrapolate microscale information within some constraints. Presumably the synoptic scale exerts considerable control for sites within several hundred kilometers. The details of the association between the synoptic scale patterns and the inversion at RNP and SHNP is currently being investigated.

The morning transition process is quite similar at both sites also. This is apparent from comparison of mean trend curves as well as the regression models. The most important local predictor of the transition time at both locations is the predawn ΔT. It is interesting that interchanging the models developed separately for each site does not always increase the forecast error. In fact, when the RNP clear day model is used to predict the SHNP transition time, the model performance actually improves.

It is not surprising that the best skill in predicting the time of inversion breakdown at both sites is evident for clear days. Here R^2 values are highest (0.76) at SHNP. Root-mean-square errors at both sites were similar, approximately 0.3 h for clear and 0.5–0.6 h. for nonclear mornings.

Observations of cloud cover were, unfortunately, not available from the sites investigated. Such information, if available at dawn would undoubtedly be useful in improving the precision of the forecast time of transition for the non-clear days. This is true because prior and conditional probabilities of cloudiness at both sites show a reasonable persistence of cloud conditions throughout most of the transition period. However, it is doubtful that a model incorporating cloud information would improve the prediction over that attained by the clear-sky model.

Acknowledgments. The authors are grateful for the support given this project by Tim Drum and Brian McFeaters of Carolina Power and Light Company, who made the data available and provided helpful information on the site instrumentation. Funding for this work was provided by the Army Research Office under project DAAG29-82-K-0183-P0002.

REFERENCES

Anderberg, M. R., 1973: *Cluster Analysis for Application.* Academic Press, 359 pp.

Baker, D. G., J. W. Enz and H. J. Paulus, 1969: Frequency, duration, commencement time and intensity of temperature inversions at St. Paul-Minneapolis. *J. Appl. Meteor.*, **8**, 747–753.

Clarke, R. H., A. J. Dyer, R. R. Brook, D. G. Reid and A. J. Troup, 1971: The Wangara experiment: Boundary layer data. CSIRO Div. Meteor. Phys., Tech. Paper No. 19, 336 pp. [NTIS No. N71-37838.]

Environ. Data Service 1968: *Climatic Atlas of the United States.* ESSA, U.S. Dept. Commerce, U.S. Govt. Printing Office, Washington, DC 20402, 80 pp.

DeMarrais, G. A., 1959: Wind-speed profiles at Brookhaven National Laboratory. *J. Meteor.*, **16**, 181–190.

——, 1961: Vertical temperature differences observed over an urban area. *Bull. Amer. Meteor. Soc.*, **8**, 548–554.

Draper, N. R., and H. Smith, 1981: *Applied Regression Analysis.* Wiley, 709 pp.

Efron, B., and G. Gong, 1983: A leisurely look at the bootstrap, the jackknife, and cross-validation. *Amer. Statist.*, **37**, 36–48.

Gill, G. C., L. E. Olsson, J. Sela and M. Suda, 1967: Accuracy of wind measurements on towers or stacks. *Bull. Amer. Meteor. Soc.*, **48**, 665–674.

Godowitch, J. M., J. K. S. Ching and J. F. Clarke, 1979: Dissipation of the nocturnal inversion layer at an urban and rural site in St. Louis, MO. *Fourth Symp. on Turbulence, Diffusion, and Air Pollution*. Reno, Amer. Meteor. Soc.

Hosler, C. R., 1961: Low-level inversion frequency in the contiguous United States. *Mon. Wea. Rev.*, **89**, 319–335.

Lenschow, D. W., B. B. Stankov and L. Mahrt, 1979: The rapid morning boundary-layer transition. *J. Atmos. Sci.*, **36**, 2108–2124.

Mahrt, L., 1981: The early evening boundary layer transition. *Quart. J. Roy. Meteor. Soc.*, **107**, 329–343.

Moses, H., and M. A. Bogner, 1967: Fifteen-year climatological summary. U.S. Atomic Energy Commission Rep. ANL-7084, Argonne National Laboratory.

Pindyck, R. S., and D. L. Rubinfeld, 1976: *Econometric Models and Economic Forecasts*. McGraw-Hill, 576 pp.

SAS Institute Inc., 1982: *SAS User's Guide: Statistics*. SAS Institute, Inc., Cary, NC 27511, 584 pp. [ISBN 0-917382-37-4.]

Singer, I. A., and G. S. Raynor, 1957: Analysis of meteorological tower data, April 1950–March 1952, Brookhaven National Laboratory. BNL 461 (T-102). 74 pp. [ASTIA Document No. AD 133806.]

Takle, E. S., 1983: Climatology of superadiabatic conditions for a rural area. *J. Climate Appl. Meteor.*, **22**, 1129–1132.

——, R. H. Shaw and H. C. Vaughan, 1976: Low level stability and pollutant-trapping potential for a rural area. *J. Appl. Meteor.*, **15**, 36–42.

Whiteman, C. D., 1982: Breakup of temperature inversions in deep mountain valley: Part I. Observations. *J. Appl. Meteor.*, **21**, 270–289.

Wolfe, J. H., 1970: Pattern clustering by multivariate mixture analysis. *Multivar. Behav. Res.*, **5**, 329–350.

Appendix II

EXPLORATION OF SYNOPTIC INFLUENCES ON INVERSION STRENGTH AND TRANSITIONS INTO THE DAYTIME BOUNDARY LAYER

by

RAYMOND B. KIESS

A thesis submitted to the Graduate Faculty of
North Carolina State University
in partial fufillment of the
requirements for the Degree of
Master of Science
DEPARTMENT OF MARINE, EARTH, AND ATMOSPHERIC SCIENCES

RALEIGH

1985

APPROVED BY:

_____ _____

_____ _____

Chairman of Advisory Committee

ABSTRACT

KIESS, RAYMOND BRIAN. Exploration of Synoptic Influences on Inversion Strength and Transitions into the Daytime Boundary Layer. (Under the direction of Allen J. Riordan.)

Synoptic influences on the inversion strength and its transition to well-mixed daytime conditions for two rural sites in the piedmont of the Carolinas for the years 1976 - 1982 were explored.

Eigenvector analysis of sea-level pressure data for the eastern third of the United States differentiated four patterns explaining 90.7% of the variance. Six more patterns were obtained by graphical averaging among the first four. These patterns represented such realistic features as the Atlantic seaboard high and the Ohio valley trough. Each day in the study was then objectively assigned a pattern through a scoring scheme. The orientation and magnitude of the geostrophic winds at each site were also used in a separate typing scheme to examine effects of the horizontal pressure gradient upon inversion strength.

Frequency analysis of inversion strength by the eigenvector patterns revealed a significant relationship between the pressure types and the inversion strength at both sites. Inversions occurred often. However, one pattern, with high pressure centered over Georgia, had the highest association with inversion occurrence, particularly

strong inversions. Patterns associated with troughs showed less of a tendency for inversion occurrence. An average correlation coefficient of 0.7 for all patterns produced evidence that the synoptic patterns influenced inversions at both sites. However, predicting one site's inversion strength based upon the other site's was only marginally useful as root mean squared errors were nearly equal to the magnitude of the inversion strength. Geostrophic wind results showed that the orientation of the horizontal pressure gradient did not have much effect, but the magnitude did. It was found that a geostrophic wind of 18 m/s corresponding to 2 mb/100 km was sufficient to prevent strong inversions at SHNP while 9 m/s was sufficient at RNP.

Examination of the eigenvalue patterns upon the daytime boundary layer transition showed that there were no large time variations on the average transition time of 1 to 3 hours to isothermal or neutral conditions between the patterns. Though different parameters such as wind speed and solar radiation showed characteristic differences in transition for each pattern, average transtion times still generally ranged in the 1 to 3 hour time span.

strong inversions. Patterns associated with troughs showed less of a tendency for inversion occurrence. An average correlation coefficient of 0.7 for all patterns produced evidence that the synoptic patterns influenced inversions at both sites. However, predicting one site's inversion strength based upon the other site's was only marginally useful as root mean squared errors were nearly equal to the magnitude of the inversion strength. Geostrophic wind results showed that the orientation of the horizontal pressure gradient did not have much effect, but the magnitude did. It was found that a geostrophic wind of 18 m/s corresponding to 2 mb/100 km was sufficient to prevent strong inversions at SHNP while 9 m/s was sufficient at RNP.

Examination of the eigenvalue patterns upon the daytime boundary layer transition showed that there were no large time variations on the average transition time of 1 to 3 hours to isothermal or neutral conditions between the patterns. Though different parameters such as wind speed and solar radiation showed characteristic differences in transition for each pattern, average transtion times still generally ranged in the 1 to 3 hour time span.

END

DTIC

7-86